NIH Public Access
Author Manuscript
Pigment Cell Melanoma Res. Author manuscript; available in PMC 2013 September 01.

Published in final edited form as:
Pigment Cell Melanoma Res. 2012 September ; 25(5): 584–591. doi:10.1111/j.1755-148X.2012.01029.x.

A BLOC-1 Mutation Screen Reveals a Novel *BLOC1S3* Mutation in Hermansky-Pudlak Syndrome Type 8 (HPS-8)

Andrew R Cullinane[1,*], **James A Curry**[1], **Gretchen Golas**[2], **James Pan**[1], **Carmelo Carmona-Rivera**[1], **Richard A Hess**[1], **James G White**[3], **Marjan Huizing**[1], and **William A Gahl**[1,2]

[1]Medical Genetics Branch, National Human Genome Research Institute, National Institutes of Health, Bethesda MD 20892, USA

[2]Intramural Office of Rare Diseases Research, Office of the Director, National Institutes of Health, Bethesda MD 20892 USA

[3]Department of Laboratory Medicine, University of Minnesota, Minneapolis, MN 55455 USA

Summary

Hermansky-Pudlak Syndrome (HPS) is a genetically heterogeneous disorder of lysosome-related organelle biogenesis and is characterized by oculocutaneous albinism and a bleeding diathesis. Over the past decade, we screened 250 patients with HPS-like symptoms for mutations in the genes responsible for HPS subtypes 1–6. We identified 38 individuals with no functional mutations, and therefore, we analyzed all 8 genes encoding the Biogenesis of Lysosome-related Organelles Complex-1 (BLOC-1) proteins in these individuals. Here we describe the identification of a novel nonsense mutation in *BLOC1S3* (HPS-8) in a 6 year-old Iranian boy. This mutation caused nonsense mediated decay of *BLOC1S3* mRNA and destabilized the BLOC-1 complex. Our patient's melanocytes showed aberrant localization of TYRP1, with increased plasma-membrane trafficking. These findings confirm a common cellular defect for HPS patients with defects in BLOC-1 subunits. We identified only 2 patients with BLOC-1 defects in our cohort, suggesting that other HPS genes remain to be identified.

Keywords

Hermansky-Pudlak Syndrome; BLOC-1; HPS-8; *BLOC1S3*

Introduction

Hermansky-Pudlak Syndrome (HPS; MIM# 203300) is a rare autosomal recessive condition characterized by reduced skin, hair and eye pigmentation and a bleeding diathesis. Occasionally, additional symptoms occur, including pulmonary fibrosis, granulomatous colitis or neutropenia (Huizing et al., 2008). To date, nine human HPS subtypes (HPS1-9) and their associated genes have been identified (Anikster et al., 2001; Cullinane et al., 2011; Dell'Angelica et al., 1999; Li et al., 2003; Morgan et al., 2006; Oh et al., 1996; Suzuki et al., 2002; Zhang et al., 2003). All of the HPS protein products are involved in the biogenesis of lysosome-related organelles such as melanosomes in melanocytes and delta granules in platelets (Huizing et al., 2008; Raposo et al., 2001; Wei, 2006), and all are components of

[*]Corresponding Author: Andrew R Cullinane, PhD, Medical Genetics Branch, NHGRI, National Institutes of Health, Bethesda, MD 20892, USA, Tel No: 301-496-9101, andrew.cullinane@nih.gov.

All authors declare no conflicts of interest.

NIH-PA Author Manuscript
NIH-PA Author Manuscript
NIH-PA Author Manuscript

NIH-PA Author Manuscript

NIH-PA Author Manuscript

NIH-PA Author Manuscript

one of four protein complexes: BLOC-1; BLOC-2; BLOC-3; or Adaptor Protein complex-3 (AP3; Dell'Angelica et al., 1999; Huizing et al., 2008; Wei, 2006).

The BLOC-1 complex contains 8 subunits: BLOS1; BLOS2; BLOS3 (HPS-8); cappuccino; dysbindin (HPS-7); muted; pallidin (HPS-9); and snapin. HPS mouse models exist with mutations in five of the eight BLOC-1 subunits (Li et al., 2004). However, relatively little is known about the intracellular function of the BLOC-1 constituents, and only three human families with BLOC-1 defects are known (Cullinane et al., 2011; Li et al., 2003; Morgan et al., 2006). Specifically, HPS-7, HPS-8 and HPS-9 involve mutations in *DTNBP1*, *BLOC1S3* and *PLDN*, respectively. Here we describe the identification of another individual with a novel nonsense mutation in *BLOC1S3*, comprising only the second mutation leading to an HPS-8 subtype (Morgan et al., 2006).

Results

Clinical Aspects of the HPS-8 Patient

The HPS-8 patient is a male born to Iranian first cousins. The boy had brown irides and nystagmus at birth with lighter skin pigment than either olive-complexioned parent (Figure 1A). His hair showed no abnormal pigment clumping under light microscopy (Figure 1B). Albinism and poor vision required corrective lenses at 3 months of age. Bilateral eye muscle surgery was performed for strabismus at 6 months. Upon admission to the NIH Clinical Center at age 6 years, visual acuity was 20/200 OD and 20/125 OS with bilateral exotropia, strabismus, and fine horizontal nystagmus. Additional findings on ophthalmologic exams included iris transillumination, moderate pallor of the optic disks, absent foveal reflexes, and decreased pigment in the periphery of the retina (Figure 1C). Easy bruisability was evident on the boy's legs, but he had no early bleeding manifestations with circumcision nor tooth eruption, despite the absence of delta granules in his platelets (Figure 1D). However, the patient did suffer minor gum bleeds with four dental fillings and was treated with desmopressin (DDAVP) after the procedures. There was no history of epistaxis, gastrointestinal bleeds, surgery or trauma necessitating platelet transfusion. There were two episodes of asthma that required treatment in the emergency room, and allergy testing revealed reactions to pollen, dust mites, eggs, salmon, and tuna. A blood smear revealed no abnormal large granules in the neutrophils of the patient (Figure 1E) and there were no reports of serious infections. However, the patient had one episode of viral pneumonia. Dermal fibroblasts and melanocytes were cultured from a skin biopsy from this patient, and a packed pellet of cultured melanocytes was notably lighter than a melanocyte pellet from a control biopsy (Figure 1F).

BLOC-1 Subunit Mutation Screen

In the last decade, we have examined more than 250 patients with HPS-like features at the NIH Clinical Center, evaluating them at the clinical, molecular and cellular levels (Huizing et al. 2008). Most patients harbored mutations in genes encoding AP-3, BLOC-2 and BLOC-3 subunits. However, in 38 patients we did not identify defects in any of the associated genes. Since only a few mutations in BLOC-1 genes have been identified, we undertook a mutation screen of the BLOC-1 genes for this cohort of 38 unclassified HPS-like patients. This screen revealed a single patient with a new sub-type of HPS (HPS-9), associated with homozygous nonsense mutations in *PLDN* encoding the BLOC-1 subunit pallidin (Cullinane et al., 2011). Furthermore, no other member of the cohort had mutations in PLDN.

NIH-PA Author Manuscript

NIH-PA Author Manuscript

NIH-PA Author Manuscript

Molecular Analysis of the HPS-8 Patient

Our mutation analysis revealed a novel *BLOC1S3* mutation: c.131C>A, p.S44X (Figure 2A). This nonsense mutation was found in the homozygous state, as expected due to the patient's consanguineous background. Consistent with this, a SNP-chip microarray confirmed several regions of extended homozygosity throughout the genome, including homozygosity in the *BLOC1S3* region on chromosome 19q13.3 (Figure 2B), consistent with the homozygous nature of the mutation.

Both cultured fibroblasts and melanocytes from the patient showed a significant reduction in *BLOC1S3* mRNA by quantitative real-time PCR (qRT-PCR), compared to control cells (Figure 3A; fibroblasts, 5.9 ± 1.2% of control; melanocytes, 4.1% ± 1.1% of control, $p<0.001$, n=3). *BLOC1S3* (GenBank accession NM_212550) is a two-exon gene, of which only exon 2 is protein coding (Figure 3B). Since the qRT-PCR Taqman assay was located entirely within exon 2, genomic DNA could also potentially be amplified, even though all RNA samples were treated with DNase. Therefore, we designed PCR primers with one primer-pair (F1-R) in the coding exon 2, and another pair with the forward primer (F2) in the non-coding exon 1 and the reverse in exon 2 (R) as before. Neither of these produced detectable *BLOC1S3* amplified cDNA in either the patient's fibroblasts or melanocytes, despite being present in control cells (Figure 3C). This suggests that nonsense mediated decay (NMD) is occurring for this mutant transcript, even though the nonsense mutation does not occur more than 55 base pairs upstream of the last exon-exon boundary of the spliced transcript, which is the usual cut off for NMD to occur (Maquat, 2004; Martina et al., 2003). Such atypical cases have been previously reported, however, and the term used for this event is boundary independent NMD (Maquat, 2004; Martina et al., 2003). In any event, since no *BLOC1S3* mRNA could be detected, very little protein, if any, is likely being synthesized.

Cellular Characterization of the HPS-8 Patient

Since no commercial antibody is available for BLOS3, we could not perform immunoblotting to detect for the absence of this protein in the HPS-8 patient. However, we and others have shown in human and mouse cells that defects in one BLOC-1 subunit destabilize the entire complex at the protein level, resulting in absence or significant down-regulation of other BLOC-1 subunits (Cullinane et al., 2011; Falcon-Perez et al., 2002; Moriyama and Bonifacino, 2002). Therefore, we subjected fibroblast lysates from control, HPS-8 and HPS-9 patients to immunoblotting with antibodies to the BLOC-1 subunits cappuccino, dysbindin (HPS-7), pallidin (HPS-9) and snapin (Figure 3D). This revealed an absence of pallidin in the HPS-9 patient, as expected, and a reduction in the HPS-8 patient (55.0% compared to control); furthermore, the cappuccino and dysbindin subunits were absent from both patients. Snapin was reduced in both BLOC-1 patients at 53.1% and 59.3% compared to control lysates for the HPS-8 and HPS-9 patients, respectively. Taken together, these data further suggest that when any one member of the BLOC-1 complex is mutated, the whole complex is unstable and prone to degradation. Consistent with previous data, the BLOC-1 patient lysates showed normal protein expression for HPS5 and HPS4, BLOC-2 and BLOC-3 subunits respectively (Figure 3E). This confirms that the BLOC-2 and BLOC-3 complexes are normally expressed and form independently in BLOC-1 deficient patients.

Early melanosomes mature into stage III melanosomes by acquiring melanogenic proteins, such as tyrosinase and TYRP1, which are crucial for melanin production and eventually produce the melanin-laden stage IV melanosomes required for pigmentation. We carried out immunofluorescence microscopy on control and patient melanocytes to test the effect of the unstable BLOC-1 complex on the ability to traffic the melanogenic proteins tyrosinase and

NIH-PA Author Manuscript

NIH-PA Author Manuscript

NIH-PA Author Manuscript

TYRP1 (mutated in OCA-1 and OCA-3, respectively) to melanosomes (Huizing et al., 2008; Raposo et al., 2001). TYRP1 abnormally accumulated in the Golgi-region in HPS-8 melanocytes, with occasional localization to non-Golgi associated punctate perinuclear structures and the plasma membrane (Figure 4A). In contrast, tyrosinase localized normally to PMEL-17 labeled structures in the HPS-8 melanocytes (data not shown) and did not appear to significantly accumulate in the Golgi-region (Figure 4B), suggesting that the mis-localization in BLOC1S3-deficient cells is cargo-specific. These findings are consistent with the situation in BLOC-1 deficient mouse melanocytes, in which immuno-electron microscopy showed normal PMEL17 and tyrosinase distribution, but abnormal TYRP1 accumulation in tubulovesicular structures and early vacuolar endosomes near the Golgi (Setty et al., 2007).

Previous studies of BLOC-1 mouse melanocytes showed enhanced flux of TYRP1 through the plasma membrane and decreased steady state TYRP1 levels due to lysosomal degradation of mis-trafficked TYRP1 (Setty et al., 2007). Our studies of HPS-8 melanocytes yielded similar results; steady state TYRP1 levels were decreased in the patient's melanocytes by immunofluorescence microscopy (Figure 4A). Furthermore, by biotinylating the surface proteins before cell lysis, TYRP1 appeared significantly increased in the patient's plasma membrane protein fraction (Figure 4C). Similar to our previous experiments in HPS-9 melanocytes, the TYRP1 on the plasma membrane showed a reduced rate of endocytosis compared to that of control cells (Figure 4D), possibly due to saturation of the endocytosis machinery by the increased TYRP1 on the membrane. From these results we conclude that patients with BLOC-1 subunit defects have a similar cellular phenotype and that aberrant TYRP1 trafficking likely contributes to the hypopigmentation of BLOC-1 patients.

Discussion

Here we report the second case of HPS-8 to date, with albinism due to aberrant melanosome biogenesis and a bleeding diathesis due to absent platelet delta granules. Our patient had no clinical signs of additional HPS subtype-specific symptoms, including neutropenia, granulomatous colitis or pulmonary fibrosis. Since some of these symptoms may develop at a later age or may be mutation-dependent, it is crucial to follow clinical signs of this patient and to identify additional patients with BLOC-1 defects. Our molecular and cellular studies indicated that our patient exhibited a homozygous nonsense mutation in *BLOC1S3*, whose protein product, BLOC1S3, is a member of the BLOC-1 complex. The aberrantly expressed BLOC1S3 in the patient's melanocytes destabilized the complex and caused mis-trafficking of TYRP1, which abnormally accumulated in the Golgi-region and cell membrane; this severely reduced pigment production. Furthermore, the data presented here are consistent with findings in the HPS-9 patient, suggesting a common cellular defect and phenotype for all patients with mutations in the genes encoding BLOC-1 subunits. An explanation for this could be that the BLOC-1 complex becomes unstable and the proteins that constitute the complex become prone to degradation once one of the subunits is absent or mutated. The absence of the Dysbindin and Cappuccino subunits in our HPS-8 (BLOS3 deficient) and HPS-9 (Pallidin deficient) patients supports this idea. However, in contrast the Snapin subunit in both patients' cells, and Pallidin in the HPS-8 patient's cells are reduced but not completely absent. The residual expression of some BLOC-1 subunits in BLOC-1 patients' cells maybe due to sub-complexes forming within the BLOC-1 complex itself, as seen in the adaptor protein complexes (Boehm and Bonifacino, 2001). Alternatively, it maybe due to the fact that members of the BLOC-1 complex, such as Pallidin and Snapin, have functions outside of the BLOC-1 complex. A structure of the BLOC-1 complex has recently been proposed based on direct protein interactions (Lee et al., 2012). However, this model does not explain the pattern of residual subunit expression in our BLOS3 or Pallidin deficient

NIH-PA Author Manuscript

NIH-PA Author Manuscript

NIH-PA Author Manuscript

cells. We therefore favor the idea that certain subunits are spared from complete degradation due to their function outside of the BLOC-1 complex.

Of our entire cohort of over 250 patients with an HPS phenotype, we had assigned an HPS subtype (HPS-1 through HPS-6) by molecular methods to all but 38 individuals. Of these 38 unclassified HPS-like patients, we identified only 2 individuals with BLOC-1 defects; they had mutations in *BLOC1S3* (HPS-8), reported here, and *PLDN* (HPS-9) reported previously (Cullinane et al., 2011). In addition to our BLOC-1 patients, there have been only 2 other families described to date that have mutations in a BLOC-1 subunit, i.e., in *DTNBP1* (HPS-7) and in *BLOC1S3* (HPS-8; (Li et al., 2003; Morgan et al., 2006). This may indicate that BLOC-1 defects are either extremely rare or embryonically lethal, or that we are not testing the correct patients for BLOC-1 defects. For example, we currently use the absence of delta granules in patients' platelets as a *sine qua non* for diagnosing HPS, but it may be that a subset of patients with BLOC-1 defects have normal platelet delta granules. In addition, due to the high expression of certain BLOC-1 subunits in the brain, and in some cases brain-specific transcripts, BLOC-1 patients might have a severe neurological phenotype in addition to classic HPS manifestations (Cullinane et al., 2011; Falcon-Perez et al., 2002). Nonetheless we still have 36 patients with HPS-like symptoms that are not HPS1 through HPS-9, and this strongly suggests that there are other, yet to be identified, genes that when mutated cause HPS. Future elucidation of genetic defects in these HPS-like patients may shine more light on these issues of variable phenotypes.

Materials and Methods

Patient

All 38 patients were enrolled in either clinical protocol NCT00001456 "Clinical and Basic Investigations Into Hermansky-Pudlak Syndrome", or protocol NCT00369421, "Diagnosis and Treatment of Inborn Errors of Metabolism and Other Genetic Disorders", approved by the NHGRI Institutional Review Board. All patients or their parents provided written, informed consent. The HPS-8 patient was enrolled in protocol NCT00001456, and written, informed consent was obtained from his parents.

Whole mount electron microscopy of platelets

Patient or control blood was mixed with citric acid dextrose (CCD) in a ratio of nine parts blood to one part anticoagulant. Platelet-rich plasma (PRP) was prepared by centrifugation at 100 RPM for 20 min at room temperature. Platelet counts and volume were determined using a Coulter HmX Hematology Analyzer (Beckman Coulter, Indianapolis, IN). When necessary, platelet counts were adjusted to 300,000 per ml. Small drops of citrate PRP were placed on formvar coated, carbon-stabilized grids (Electron Microscopy Sciences, Hatfield, PA) and rinsed with drops of sterilized water, dried from the edges with filter paper, and air-dried to remove residual moisture. The grids were examined without fixation or staining in a Philips 301 electron microscope (FEI, Hillsboro, OR).

Tissue culture

Primary patient and control fibroblasts and melanocytes were cultured from a forearm skin biopsy. Fibroblasts were grown in high-glucose (4.5 g/L) DMEM supplemented with 10% fetal calf serum (FCS; Gemini Bio-Products, West Sacramento, CA), 2 mM L-glutamine, MEM nonessential amino acid solution and penicillin-streptomycin. Melanocytes were cultured in Ham's F10 (Invitrogen, Carlsbad, CA), supplemented with 5% FCS, 5 μg/L basic fibroblast growth factor (Sigma, St. Louis, MO), 10 μg/L endothelin (Sigma), 7.5 mg/L 3-isobutyl-1-methylxanthine (Sigma), 30 μg/L choleratoxin (Sigma), 3.3 μg/L phorbol

NIH-PA Author Manuscript

NIH-PA Author Manuscript

NIH-PA Author Manuscript

12-myristate 13-acetate (Sigma), 10 mL pen/strep/glutamine (Invitrogen) and 1 mL fungizone (Invitrogen).

gDNA analysis: sequencing and SNP-array

For BLOC-1 subunits' gDNA sequencing, primers were designed to cover all coding exons and flanking intronic regions of *BLOC1S1* (NT_029419.12), *BLOC1S2* (NT_030059.13), *BLOC1S3* (NT_011109.16), *CNO* (NT_006051.18), *DTNBP1* (NT_007592.15), *MUTED* (NT_007592.15), *PLDN* (NT_010194.17) and *SNAPIN* (NT_004487.19); primer sequences available on request. Direct sequencing was carried out using the di-deoxy termination method (ABI BigDye Terminator v3.1) on an ABI 3130xl DNA sequencer (Applied Biosystems, Austin, TX). Results were analyzed using Sequencher v4.9 software (Gene Codes Corporation, Ann Arbor, MI). The HPS-8 patient's *BLOC1S3* mutation was verified bi-directionally based on accession number NM_212550.3. For SNP genotyping, genomic DNA was run on a Human 1M-Duo DNA Analysis BeadChip and the data analyzed using the GenomeStudio software (both Illumina, San Diego, CA).

RNA analysis: extraction, cDNA and qRT-PCR

Total RNA was isolated from control and patient fibroblasts and melanocytes using RNA-Easy Mini-Kit (Qiagen) according to the manufacturer's protocol. RNA was treated with a DNase kit (DNA-free) to remove all remaining DNA according to the manufacturer's protocol (Applied Biosystems, Austin, TX). RNA concentrations and purity were measured on the Nanodrop ND-1000 apparatus (Nanodrop Technologies, Wilmington, DE). First strand cDNA was synthesized using a high capacity RNA-to-cDNA kit (Applied Biosystems) according to the manufacturer's guidelines. For q-RT-PCR, Taqman gene expression master mix reagent and Assays-On-Demand (Applied Biosystems) were obtained for *BLOC1S3* (Assay ID Hs03028695_s1) and a control gene, *GAPDH* (Assay ID Hs99999905_m1). Q-RT-PCR was performed using 100 ng cDNA, on an ABI PRISM 7900 HT Sequence Detection System (Applied Biosystems) using the comparative C_T method ($\Delta\Delta C_T$); this method measures relative gene expression (Livak and Schmittgen, 2001). The cycling conditions were as follows: 2 min at 50°C, 10 min at 95°C, and 40 cycles at 95° C for 15 s and 60° C for 60 s. For PCR on cDNA a primer pair (F1-R) was designed entirely within the coding exon of *BLOC1S3* and a second pair (F2-R) with the forward primer in the *BLOC1S3* non-coding exon 1 and the same reverse primer as before. PCR was performed on cDNA for both primer pairs and a *GAPDH* primer pair as a control. Products were run on 2% agarose gels.

Antibodies

Mouse monoclonal antibodies against the following proteins were acquired as follows: β-actin (Clone AC-15; Sigma Aldrich, St Louis MO), TYRP1 (used for immunofluorescence and internalization assay; clone TA99, ATCC, Manassas, VA), tyrosinase (clone T311) and cappuccino (Clone S-5; both Santa Cruz Biotechnology, Santa Cruz, CA). Rabbit polyclonal antibodies against the following proteins were acquired as follows: TYRP1 (used for immunoblotting) and HPS4 (both Santa Cruz Biotechnology, Santa Cruz, CA); HPS5 and snapin (both ProteinTech, Chicago, IL). The goat polyclonal antibody against Dysbindin was purchased from Santa Cruz Biotechnology, and a sheep polyclonal antibody against TGN46 was obtained from AbD Serotec (Raleigh, NC). The mouse monoclonal antibody against pallidin was a kind gift from Dr. E. Dell'Angelica (UCLA School of Medicine, Los Angeles, CA).

NIH-PA Author Manuscript

NIH-PA Author Manuscript

NIH-PA Author Manuscript

Protein extraction and immunoblotting

Cells were grown to confluency in 75-cm^2 flasks, washed twice with ice-cold PBS and scraped into 250 μL of cell lysis buffer containing 50 mM Tris-HCl (at pH7.5), 50 mM sodium fluoride, 5 mM sodium pyrophosphate, 1 mM sodium orthovanadate, 1 mM EDTA, 1 mM EGTA, 0.27 M sucrose, 1% Triton X-100 and Complete, Mini Protease Inhibitor Cocktail (Roche Diagnostics). Cell lysates were centrifuged (15,000 RPM, for 15 min at 4°C); supernatants were removed for immunoblotting. Twenty micrograms of total protein, as determined by the Dc Protein assay (BioRad, Hercules, CA), were loaded onto 4–12% Tris-Glycine gels. For HRP detection, proteins were blotted onto PVDF membranes, or nitrocellulose membranes for Li-Cor detection, using the iBlot transfer system (Invitrogen). After blotting, membranes were probed with the appropriate antibodies and loading was controlled by blotting the same membranes with β-actin. HRP-conjugated secondary anti-mouse or anti-rabbit antibodies (Amersham Biosciences, Piscataway, NJ) and IRDye 800CW conjugated secondary anti-mouse or anti-rabbit antibodies (Li-Cor Biosciences, Lincoln, NE) were used. The antigen–antibody complexes were visualized with an Enhanced Chemiluminescence (ECL) kit (Amersham Biosciences, Piscataway, NJ) or detected using the Li-Cor Odyssey Infrared imaging system. All blots were detected using HRP except for HPS5 and β-actin when appropriate, where Li-Cor detection was used.

Plasma-membrane protein biotinylation

For membrane protein biotinylation, control and patient melanocytes were incubated with 500 μL of 0.25 mg/mL EZ-Link Sulfo-NHS-SS-Biotin (Thermo Scientific, Waltham, MA) for 30 mins at 4°C. This reaction was quenched by incubating with 1 M NH_4Cl for 5 min. Protein was then extracted using the protocol above. The biotin-labeled proteins were separated from the total lysates using streptavidin Dynabeads (Invitrogen, Carlsbad, CA) according to the manufacturer's instructions. The protein samples were loaded directly onto SDS-PAGE gels for immunoblotting analysis.

Immunofluorescence microscopy

Cells were grown in 4-well chamber slides and fixed using 4% paraformaldehyde and permeabilized using 0.1% Triton-X-100. Alexafluor 488 and 555 secondary antibody conjugates were purchased from Invitrogen (Carlsbad, CA), and nuclei were counterstained with DAPI (Vector Laboratories, Burlingame, CA). Cells were imaged with a Zeiss 510 META confocal laser-scanning microscope with the pinhole set to 1 Airy unit. A series of optical sections were collected from the *xy* plane and merged into maximum projection images.

TYRP1 internalization assay

This assay was carried out essentially as previously described (Setty et al., 2007). Briefly, control and HPS-8 patient melanocytes were trypsinized and washed twice with Ham's F10 medium containing 10% FBS and 25mM HEPES. For each time point, 2×10^5 cells were used and incubated with a monoclonal antibody against TYRP1 on ice for 30 min to allow antibody binding to plasma membrane TYRP1. Cells were then washed twice with medium and transferred to 37°C for different amounts of time (0, 5, 10, 15, 30, 60 min), after which they were incubated on ice with Alexafluor 488 conjugated secondary antibodies for 30 min. The cells were then washed twice with medium and re-suspended in FACS buffer (5% FBS, I mM EDTA in 1x PBS). The samples were sorted on a Becton Dickenson FACSCalibur flow cytometer and green fluorescence quantified and analyzed using FlowJo software.

NIH-PA Author Manuscript

NIH-PA Author Manuscript

NIH-PA Author Manuscript

Acknowledgments

We appreciate the excellent technical assistance of Roxanne Fischer and Carla Ciccone. We thank Dr. Thomas Markello for assistance with SNP arrays, and Dr. E. Dell'Angelica for supplying the pallidin antibody. This study was supported by the Intramural Research Program of the National Human Genome Research Institute, National Institutes of Health, Bethesda, MD, USA.

References

Anikster Y, Huizing M, White J, Shevchenko YO, Fitzpatrick DL, Touchman JW, Compton JG, Bale SJ, Swank RT, Gahl WA, et al. Mutation of a new gene causes a unique form of Hermansky-Pudlak syndrome in a genetic isolate of central Puerto Rico. Nat Genet. 2001; 28:376–80. [PubMed: 11455388]

Boehm M, Bonifacino JS. Adaptins: the final recount. Mol Biol Cell. 2001; 12:2907–20. [PubMed: 11598180]

Cullinane AR, Curry JA, Carmona-Rivera C, Summers CG, Ciccone C, Cardillo ND, Dorward H, Hess RA, White JG, Adams D, et al. A BLOC-1 Mutation Screen Reveals that PLDN Is Mutated in Hermansky-Pudlak Syndrome Type 9. Am J Hum Genet. 2011; 88:778–87. [PubMed: 21665000]

Dell'angelica EC, Shotelersuk V, Aguilar RC, Gahl WA, Bonifacino JS. Altered trafficking of lysosomal proteins in Hermansky-Pudlak syndrome due to mutations in the beta 3A subunit of the AP-3 adaptor. Mol Cell. 1999; 3:11–21. [PubMed: 10024875]

Falcon-Perez JM, Starcevic M, Gautam R, Dell'angelica EC. BLOC-1, a novel complex containing the pallidin and muted proteins involved in the biogenesis of melanosomes and platelet-dense granules. J Biol Chem. 2002; 277:28191–9. [PubMed: 12019270]

Huizing M, Helip-Wooley A, Westbroek W, Gunay-Aygun M, Gahl WA. Disorders of lysosome-related organelle biogenesis: clinical and molecular genetics. Annu Rev Genomics Hum Genet. 2008; 9:359–86. [PubMed: 18544035]

Lee HH, Nemecek D, Schindler C, Smith WJ, Ghirlando R, Steven AC, Bonifacino JS, Hurley JH. Assembly and architecture of biogenesis of lysosome-related organelles complex-1 (BLOC-1). J Biol Chem. 2012; 287:5882–90. [PubMed: 22203680]

Li W, Rusiniak ME, Chintala S, Gautam R, Novak EK, Swank RT. Murine Hermansky-Pudlak syndrome genes: regulators of lysosome-related organelles. Bioessays. 2004; 26:616–28. [PubMed: 15170859]

Li W, Zhang Q, Oiso N, Novak EK, Gautam R, O'brien EP, Tinsley CL, Blake DJ, Spritz RA, Copeland NG, et al. Hermansky-Pudlak syndrome type 7 (HPS-7) results from mutant dysbindin, a member of the biogenesis of lysosome-related organelles complex 1 (BLOC-1). Nat Genet. 2003; 35:84–9. [PubMed: 12923531]

Livak KJ, Schmittgen TD. Analysis of relative gene expression data using real-time quantitative PCR and the 2(-Delta Delta C(T)) Method. Methods. 2001; 25:402–8. [PubMed: 11846609]

Maquat LE. Nonsense-mediated mRNA decay: splicing, translation and mRNP dynamics. Nat Rev Mol Cell Biol. 2004; 5:89–99. [PubMed: 15040442]

Martina JA, Moriyama K, Bonifacino JS. BLOC-3, a protein complex containing the Hermansky-Pudlak syndrome gene products HPS1 and HPS4. J Biol Chem. 2003; 278:29376–84. [PubMed: 12756248]

Morgan NV, Pasha S, Johnson CA, Ainsworth JR, Eady RA, Dawood B, Mckeown C, Trembath RC, Wilde J, Watson SP, et al. A germline mutation in BLOC1S3/reduced pigmentation causes a novel variant of Hermansky-Pudlak syndrome (HPS8). Am J Hum Genet. 2006; 78:160–6. [PubMed: 16385460]

Moriyama K, Bonifacino JS. Pallidin is a component of a multi-protein complex involved in the biogenesis of lysosome-related organelles. Traffic. 2002; 3:666–77. [PubMed: 12191018]

Oh J, Bailin T, Fukai K, Feng GH, Ho L, Mao JI, Frenk E, Tamura N, Spritz RA. Positional cloning of a gene for Hermansky-Pudlak syndrome, a disorder of cytoplasmic organelles. Nat Genet. 1996; 14:300–6. [PubMed: 8896559]

NIH-PA Author Manuscript

NIH-PA Author Manuscript

NIH-PA Author Manuscript

Raposo G, Tenza D, Murphy DM, Berson JF, Marks MS. Distinct protein sorting and localization to premelanosomes, melanosomes, and lysosomes in pigmented melanocytic cells. J Cell Biol. 2001; 152:809–24. [PubMed: 11266471]

Setty SR, Tenza D, Truschel ST, Chou E, Sviderskaya EV, Theos AC, Lamoreux ML, Di Pietro SM, Starcevic M, Bennett DC, et al. BLOC-1 is required for cargo-specific sorting from vacuolar early endosomes toward lysosome-related organelles. Mol Biol Cell. 2007; 18:768–80. [PubMed: 17182842]

Suzuki T, Li W, Zhang Q, Karim A, Novak EK, Sviderskaya EV, Hill SP, Bennett DC, Levin AV, Nieuwenhuis HK, et al. Hermansky-Pudlak syndrome is caused by mutations in HPS4, the human homolog of the mouse light-ear gene. Nat Genet. 2002; 30:321–4. [PubMed: 11836498]

Wei ML. Hermansky-Pudlak syndrome: a disease of protein trafficking and organelle function. Pigment Cell Res. 2006; 19:19–42. [PubMed: 16420244]

Zhang Q, Zhao B, Li W, Oiso N, Novak EK, Rusiniak ME, Gautam R, Chintala S, O'brien EP, Zhang Y, et al. Ru2 and Ru encode mouse orthologs of the genes mutated in human Hermansky-Pudlak syndrome types 5 and 6. Nat Genet. 2003; 33:145–53. [PubMed: 12548288]

NIH-PA Author Manuscript

NIH-PA Author Manuscript

NIH-PA Author Manuscript

Significance

Hermansky-Pudlak Syndrome (HPS) is caused by mutations in genes whose protein products are involved in the biogenesis of lysosome related organelles, such as melanosomes in melanocytes and delta granules in platelets. These proteins belong to 4 complexes, Biogenesis of Lysosome related Organelle Complex (BLOC) −1, −2, −3 and Adaptor Protein complex 3 (AP3). Mutations in genes that encode the BLOC-1 subunit proteins are rare, with only 3 mutations identified in 3 genes (*DTNBP1*,*BLOC1S3* and *PLDN*). Here we report a fourth individual with a BLOC-1 defect involving a novel mutation in *BLOC1S3;* this represents only the second identified HPS-8 patient.

NIH-PA Author Manuscript

NIH-PA Author Manuscript

NIH-PA Author Manuscript

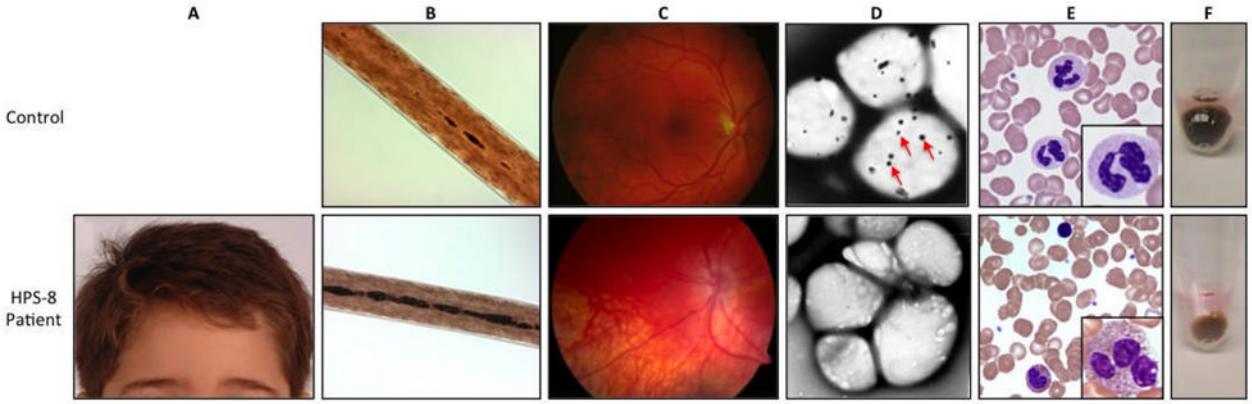

Figure 1.

Clinical aspects of HPS-8 (bottom panels) compared with controls (top panels). (A) The patient has fair skin and hair compared to other family members. (B) The patient's hair shaft shows significant pigmentation compared to that a dark haired/ethnically matched control, and no abnormal pigment clumping. (C) The patient has decreased retinal pigment in the periphery compared to control. (D) Whole-mount electron microscopy of the patient's platelets revealed no delta granules, which are present in control platelets (arrows). (E) A blood smear revealed no abnormal large granules in the neutrophils. (F) Packed melanocytes show reduced pigment in the HPS-8 patient compared to a matched control.

NIH-PA Author Manuscript

NIH-PA Author Manuscript

NIH-PA Author Manuscript

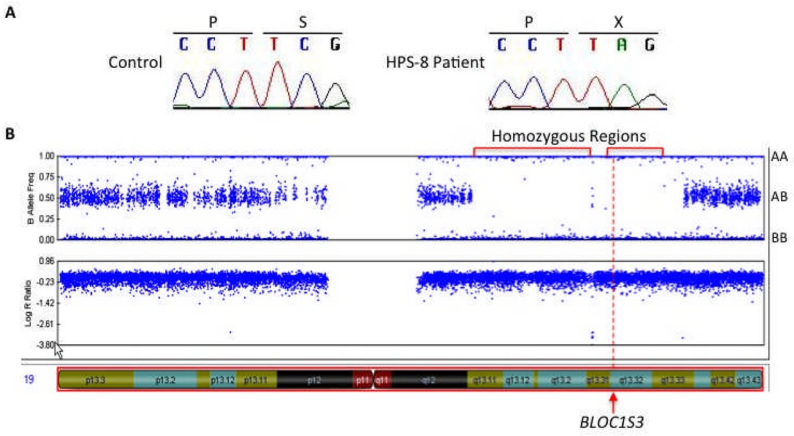

Figure 2.

Molecular studies in the HPS-8 patient. (A) Sequencing chromatograms from control and patient genomic DNA. The patient is homozygous for c.131C>A in *BLOC1S3* causing p.S44X at the protein level. (B) SNP-array data of chromosome 19 for the HPS-8 patient. The vertical red dotted line shows the position of *BLOC1S3* and the red brackets show extended regions of homozygosity (top plot). On the B allele plot (upper chart), the middle dots represent heterozygous SNPs (AB), and the top and bottom borders represent homozygous SNPs (AA or BB). The log R ratio plot (lower chart) shows that there are normal SNP calls in both homozygous regions, indicating that no deletions or insertions are present.

NIH-PA Author Manuscript

NIH-PA Author Manuscript

NIH-PA Author Manuscript

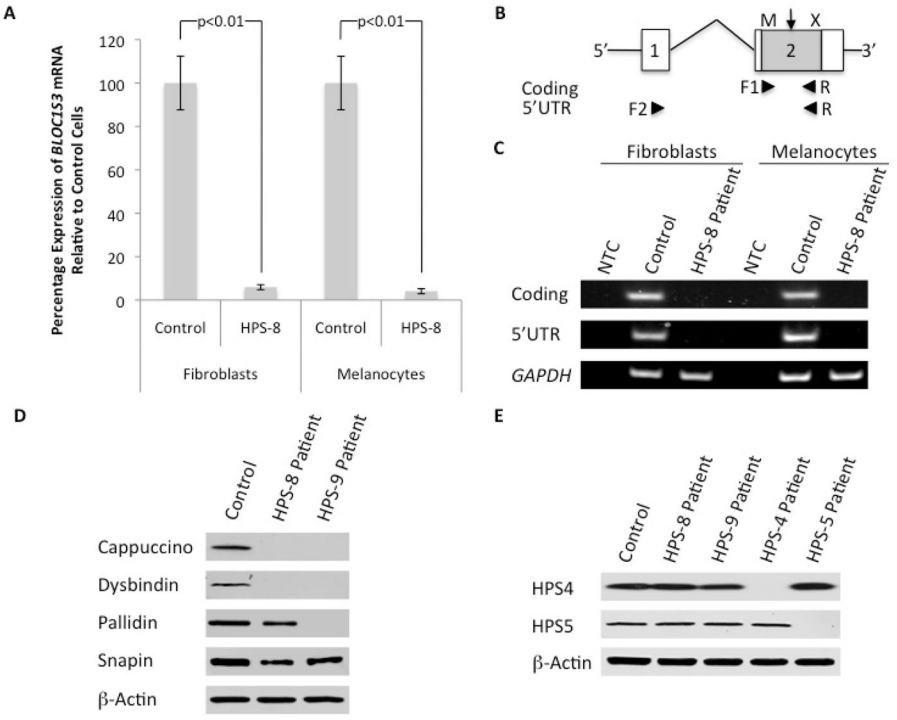

Figure 3.

BLOC1S3 mRNA and protein analysis of HPS-8 cells. (A) Quantitative real-time PCR results for *BLOC1S3* mRNA expression in patient compared to control fibroblasts and melanocytes. Values shown are percentage expression of *BLOC1S3* in patient cells compared to control cells, normalized by *GAPDH* (Error bars = ± 1 SEM, n=3, $p<0.001$). (B) Schematic diagram depicting the exon structure of *BLOC1S3*, where only exon 2 is protein coding, and contains both the start (ATG; M) and stop (X) codons (grey box). Arrowheads show the position of the PCR primer used for (C) and arrow shows position of the HPS-8 patient's mutation. (C) Standard PCR on cDNA of control and patient's fibroblasts or melanocytes. Agarose gel images of PCR products show no detectable *BLOC1S3* amplification in patient's cDNA for either primer set (coding: F1-R; 5′UTR: F2-R); *GAPDH* was amplified. NTC, non-template control. (D) Immunoblots of fibroblast extracts from the HPS-8 patient and the previously reported HPS-9 patient for the BLOC-1 subunits cappuccino, dysbindin, pallidin and snapin. Cappuccino and dysbindin (and pallidin in the HPS-9 patient) are undetectable. Pallidin is reduced in the HPS-8 patient and snapin is also reduced in both BLOC-1 patients. (E) Immunoblots of lysates from HPS-8 and HPS-9 (BLOC-1), HPS-4 (BLOC-3) and HPS-5 (BLOC-2) patients using antibodies to the HPS4 and HPS5 proteins, showing independent assembly of the BLOC complexes. Loading was controlled by immunoblotting the same membrane for β-actin.

NIH-PA Author Manuscript

NIH-PA Author Manuscript

NIH-PA Author Manuscript

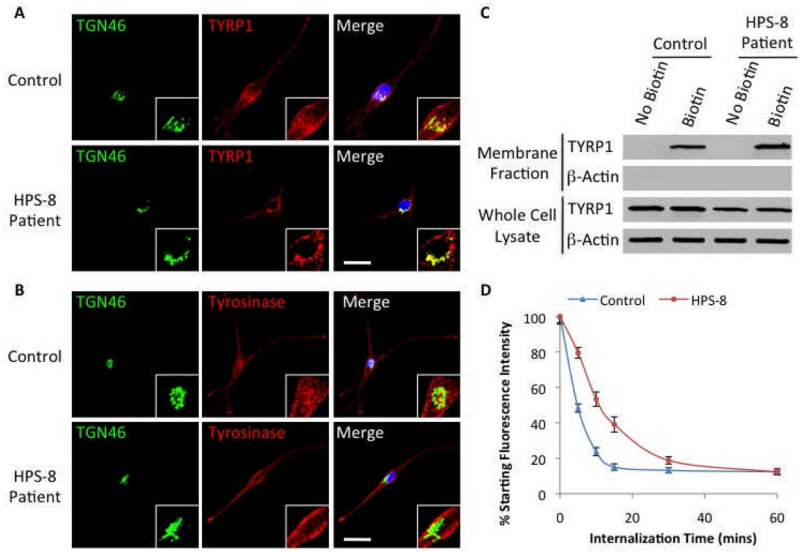

Figure 4.

Common defect of TYRP1 trafficking in BLOC-1 patients. (A) Confocal immunofluorescence images showing TYRP1 in the dendrites and tips of control melanocytes while in the HPS-8 cells the TYRP1 appears to be more perinuclear, in the plasma membrane, and co-localizes with the Golgi (inserts). (B) Tyrosinase localization appears normal in the HPS-8 patients' melanocytes and is comparable with control cells. Golgi marked by TGN46, nuclei stained with DAPI and scale bar represents 20μm. (C) Plasma membrane biotinylation assay shows increased TYRP1 protein on the membrane of the HPS-8 patients cells compared to control cells despite there being less TYRP1 in the whole cell lysate from the patient. Blotting the same membrane for β-actin demonstrates purity of the membrane fraction, and equal loading of the whole cell lysate. (D) TYRP1 internalization assay shows a decreased rate of endocytosis from the plasma membrane in the HPS-8 patient cells compared to that of control. Values shown are percentage of starting TYRP1 on the plasma membrane (error bars = ± 1 SEM, n=3).